



Hydrology, Environment (Hydrology, Hydrogeology)

Experimental monitoring and numerical study of pesticide (carbofuran) transfer in an agricultural soil at a field site

Abderrahim Hmimou^{a,*}, Abdellatif Maslouhi^a, Karim Tamoh^b, Lucila Candela^b^a *Laboratoire interdisciplinaire en ressources naturelles et en environnement, faculté des sciences, université Ibn-Tofail, BP 133, 14000 Kénitra, Morocco*^b *Department of geotechnical engineering and geosciences, technical university of Catalonia, UPC, Barcelona, Spain*

ARTICLE INFO

Article history:

Received 3 December 2013

Accepted after revision 13 March 2014

Available online 16 September 2014

Keywords:

Carbofuran

Bromide

Agricultural plot

Transport

Infiltrometer

Mechanistic model

ABSTRACT

We studied the transport of a pesticide at field scale, namely carbofuran molecule, which is known for its high mobility, especially in sandy soils with high hydraulic conductivity and low organic matter. To add to our knowledge of the future of this high-mobility molecule in this type of soils, we developed a mechanistic numerical model allowing the simulation of hydric and solute transfers (bromide and carbofuran) in the soil. We carried out this study in an agricultural plot in the region of Mnasra in Morocco. Confrontation of the measured and simulated values allowed the calibration of the parameters of hydric transfer and carbofuran. The developed model accurately reproduces the measured values. Despite a weak irrigation and precipitation regime, carbofuran was practically leached beyond the root zone. Prospective simulations show that under a more important irrigation regime, carbofuran reaches a 100-cm depth, whereas it does not exceed 60 cm under a deficit regime.

© 2014 Académie des sciences. Published by Elsevier Masson SAS. All rights reserved.

1. Introduction

Groundwater reserves are important exploitable water resources. Unfortunately, the intensive agriculture practised today requires the use of fertilizers and pesticides in large quantities and, sometimes, in an uncontrolled way, and significantly reduces the quality of groundwater (Ibnoussina et al., 2006; Laftouhi et al., 2003; Saâdi et al., 1999; Teijón et al., 2010; Worrall and Kolpin, 2004).

To control the potential contamination of groundwater by pesticides, it is essential to understand the transport process involved (Kodešová et al., 2011). The approaches used include a field study conducted in natural agro-pedoclimatic conditions (Candela and Mariñó, 2004; Rekolainen

et al., 2000), and a simulation using mathematical models (Beven, 2012).

Russo et al. (1994) studied the effects of variations of the soil water content on pesticides leaching in agricultural unsaturated zones. Kuntz and Grathwohl (2009) studied the simulation of pollutant flow and transport of two reactive compounds, i.e., lindane and phenanthrene, in a column of the unsaturated zone. They were interested in the validity of the hypothesis of a continuous stream percolation in the deterministic models, from local to larger scales.

Our study is focused on the modelling of transport of carbofuran, which is a broad-spectrum insecticide–nematicide that belongs to the carbamates chemical family. Carbofuran gives rise to harmful effects on human health and environment. Several previous studies showed that the mobility of carbofuran in a sandy soil was lower in organic matter, and presents an environmental problem, such as high potential leaching (Dahchour, 1995; Krishna and Philip, 2008). According to its mobility index

* Corresponding author.

E-mail address: hmimou@gmail.com (A. Hmimou).

(GUS = 3.75, Gustafson, 1989), this pesticide is leached easily after a heavy rainfall or a repetitive irrigation (Dahchour, 1995; El Mrabet, 2002). However, results of soil column suggest that there are real possibilities for carbofuran to reach relatively deep aquifers (Moreal and Van bladel, 1983).

To understand the mechanisms of this substance transport in sandy soils, and to study its impact on groundwater contamination, we carried out an experimental study of the water movement and the transport of both carbofuran and an anionic tracer flow (KBr) (Hmimou et al., 2011), on the bare soil of an experimental plot in the Mnasra region (Morocco). Particular attention was paid to the unsaturated soil, the location of the main flow and the transport process. On the other hand, to better evaluate the risk of groundwater contamination by carbofuran, we used a mechanistic mathematical model developed by the Interdisciplinary Laboratory Environment and Natural Resources (LIRNE) and validated on experimental data collected from the study site. It should be noted that the degradation products of carbofuran were not traced.

The developed model can reproduce the fate of carbofuran in the unsaturated zone, depending on the irrigation system used. Such simulations need an advanced hydrodynamic characterization of the soil. Hence, we carried out negative charge infiltration experiments at several locations in the experimental station (Perroux and White, 1988; Tamoh and Maslouhi, 2004).

2. Materials and methods

2.1. Study area

The study area is the experimental station (CDA 236) located in the Mnasra area, about 30 km north of the city of Kenitra, in northwestern Morocco (Fig. 1).

Mnasra region is a strip of land parallel to the Atlantic coast, of about 50,000 ha, located on the right bank of the Sebou River, 7 to 14 km wide and over about 50 km in length extending from the North of the Kenitra City. It is characterized by a diversity of crops, such as cereals, sugar beet, fodder and vegetables. The experimental site is equipped with a weather station that provided various data, such as rainfall and minimum and maximum temperatures (Fig. 1).

2.2. Description of experiments

The experiment was carried out on a 200-m² field with flat topography, subdivided into ten basic 4 × 5 m² plots. This study is focused on uncultivated plots on which are

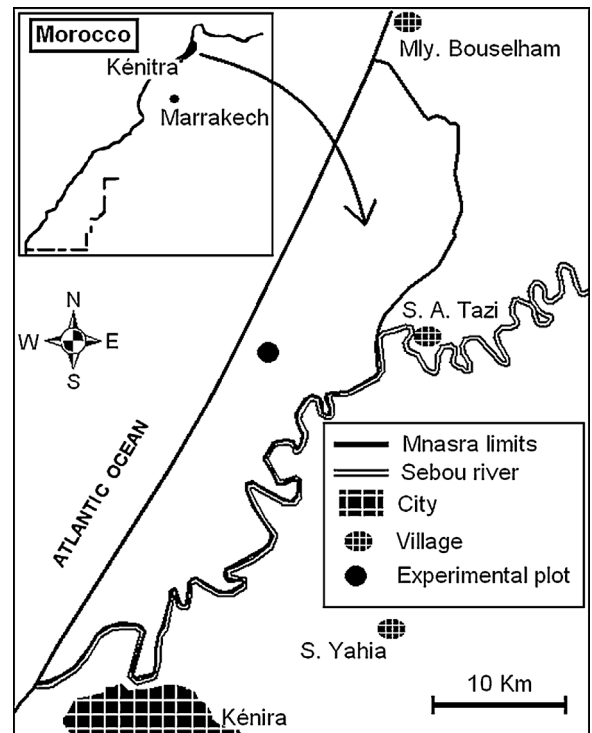


Fig. 1. The Mnasra region showing the studied site location.

applied a Br and carbofuran flow tracer, and on an uncultivated and untreated control plot.

The site sandy soil was classified as an Alfisol, according to U S Soil Taxonomy (Soil Survey and Staff, 1999) and a sandy loam according to the USDA (USDA-SCS, 1975). Its physicochemical characteristics are presented in Table 1.

The tracer used is an anionic tracer (Br⁻) form (KBr). It was applied with a dose of 61.77 g/m². The carbofuran C₁₂H₁₅NO₃ (2,3-dihydro-2,2-dimethylbenzofuran-7-yl-N-methyl carbamate) of the commercial product Furadan was applied with a dose of 4 g/m² based on active ingredient. Carbofuran has a solubility of 700 mg/L and a low vapor pressure, i.e., 3.41 × 10⁻⁶ mmHg at 25 °C. The half-life of carbofuran reaches values ranging from 25.7 to 107 days in soils with pH values and temperatures close to those of our experiments (El Mrabet, 2002). An injection mode was used in a slot corresponding to the injection of a constant concentration for a certain time. Spatial variability was considered by many measurement reiterations on average three times. The solutes were injected using a pulverizer, advancing at a constant speed while keeping the same nozzle flow rates to ensure a homogeneous application. The application of solutes was followed by a first irrigation during the monitoring period. The cumulative amounts of precipitation and irrigation were 62 mm and 160 mm, respectively. Irrigation was carried out with a sprinkler. Evapotranspiration was calculated on a daily basis from observed *in situ* data.

The spatio-temporal monitoring of physical and chemical parameters, such as humidity, temperature, bromide and pesticide concentrations in the soil was conducted for 90 days.

Table 1
Physicochemical characteristics of the soil.

Depth (cm)	pH	Organic matter (%)	Clay (%)	Loam (%)	Sand (%)	Bulk density (g·cm ⁻³)
0–20	7.04	1.41	10.00	7.45	82.75	1.55
20–40	6.97	0.62	9.65	7.95	82.36	1.76
40–60	7.59	0.58	9.20	8.60	82.40	1.69

Samples were collected using an auger from the following depths: 0–20 cm, 20–40 cm and 40–60 cm. No trace of carbofuran or bromide was detected at all levels before treatment.

Determination of bromide in soil samples was carried out by ion chromatography using a Metrohm 881 Compact IC Pro, with a detection limit of 0.1 mg/L (Tirumalesh, 2008).

It should be noted that another method of bromide analysis was carried out by XRF following the procedure of Margui et al. (2009). The comparison between the two methods was statistically evaluated, leading to similar results (Hmimou et al., 2011).

The carbofuran was analyzed by liquid chromatography using a HPLC device: LCQ Advantage Max, Brand Thermo Electron equipped with a type BDS Hypersil C18 (150 × 4, 6 mm × 5 μm) column.

2.3. Hydrodynamic characterization

The hydrodynamic characterization of the plot soil is performed *in situ* using a disc infiltrometer with the negative charge method. Several infiltration measurements are conducted. For the retention curve $h(\theta)$, we use the expression of Van Genuchten (1980):

$$\theta(h) = \theta_r + (\theta_s - \theta_r) \left(1 + \left(\frac{h}{h_g} \right)^n \right)^{-m} \quad (1)$$

where h is the water pressure head, θ_s the saturation water content ($L^3 L^{-3}$), a structure parameter h_g (L), θ_r the residual water content ($L^3 L^{-3}$), n and m are shape parameters, such as $m = 1 - 2/n$. Performing several measurements at different pressures, we could reconstitute a part of the retention curve $\theta(h)$. For hydraulic conductivity K , we used the model of Brooks and Corey (Brooks and Corey, 1964):

$$K(h) = K_s \left(1 + \left(\frac{h}{h_g} \right)^n \right)^{-m\eta} \quad (2)$$

where K represents the saturated hydraulic conductivity ($L T^{-1}$) and η a shape parameter.

2.4. Flow and transport model

Water movement in the unsaturated soil can be described by Richard's equation as follows:

$$C(h) \frac{\partial h}{\partial t} = \frac{\partial}{\partial z} \left[K(h) \left(\frac{\partial h}{\partial z} - 1 \right) \right] - \frac{ETR}{Z_{evap}} \quad (3)$$

with $C(h) = \frac{d\theta}{dh}$ the capillary capacity of soil (L^{-1}), h is the soil water pressure (L), θ is the volumetric water content ($L^3 L^{-3}$), K is hydraulic conductivity ($L T^{-1}$), z is the spatial coordinate, positive downward (L), t is time (T), ETR is the actual evapotranspiration ($L T^{-1}$), and Z_{evap} is the depth affected by evaporation ($Z_{evap} = 10$ cm).

The transport of an interactive and non-conservative solute in the vadose zone is described on the basis of the advection–dispersion equation assumed in the model. It also incorporates a homogeneous reaction, i.e., pesticide

degradation described by first-order kinetics:

$$R\theta \frac{\partial C}{\partial t} = \frac{\partial}{\partial z} \left[\theta D_a(\theta) \frac{\partial C}{\partial z} \right] - q_z \frac{\partial C}{\partial z} - \mu\theta C \quad (4)$$

$$R = 1 + \frac{\rho K_d}{\theta} \text{ and } \mu = \mu_w + \frac{\rho K_d}{\theta} \mu_s, \quad (5)$$

where R is the retardation factor, a dimensionless quantity, C is the solute concentration ($M L^{-3}$), D_a is the apparent hydrodynamic dispersion coefficient ($L^2 T^{-1}$), q_z is the Darcian water flux (LT^{-1}), μ is the degradation coefficient (T^{-1}), ρ is the bulk density of the porous medium ($M L^{-3}$), K_d is the distribution coefficient ($L^3 M^{-1}$), μ_w and μ_s are the degradation constants in the solid and the liquid phase, respectively.

Before the beginning of the experiment, we measured the water contents for each soil profile, since we are dealing with a homogeneous soil. Consequently, we can define an initial uniform water content profile with an average value of $\theta_0 = 0.11 \text{ cm}^3/\text{cm}^3$. The solute is not present initially in the field. The initial conditions are expressed as:

$$h(t, z) = h(\theta_0) = h(0.11) = -161.3 \text{ cm} \quad t = 0 \text{ and } 0 \leq z \leq z_{max} \quad (6)$$

$$C(t, z) = 0 \quad t = 0 \text{ and } 0 \leq z \leq z_{max} \quad (7)$$

At the upper boundary of the flow model, we applied a Neuman type flux boundary condition:

$$q_0 = K(h(t, 0)) \left(1 - \frac{\partial h}{\partial z} \Big|_{z=0} \right) \quad t > 0 \text{ and } z = 0 \quad (8)$$

with: $q_0 = PI$ (9) where PI is the precipitation and/or irrigation.

At the upper boundary of the transport model, the total advective and dispersive mass fluxes of solutes were prescribed as functions of time:

$$J_0(t) = q(t, 0)C(t, 0) - \lambda |q(t, 0)| \frac{\partial C}{\partial z} \Big|_{z=0} \quad (10)$$

where $J_0(t)$ is the mass flux of solute injected in form of slot, $q(t, 0)$ the water flux density at the soil surface, and λ the dispersivity.

For the lower limit, we consider a gravity flow condition:

$$q(t, z_{max}) = K(h(t, z_{max})) \quad (11)$$

The solute convective flux is, in this limit, expressed by:

$$J(t, z_{max}) = q(t, z_{max}) \cdot C(t, z_{max}) \quad (12)$$

Richard equations and advection–dispersion equation (ADE) (Eqs. (3) and (4)) accompanied by their initial and boundary conditions were solved by a numerical finite difference scheme (Crank–Nicolson). Once all discretisations were established, a tridiagonal, and symmetric linear system of equations is obtained, which was resolved by the (SOR) algorithm. The non-linearity of equation (3) was resolved by initializing, at each time step t_i , the $c(h)$ term at time t_i , and then doing as many iterations as necessary to reach an invariable solution.

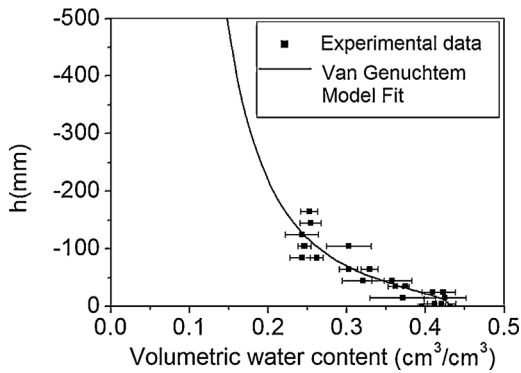


Fig. 2. Suction curve for the studied soil.

At each time step, we resolved first equation (3), and then we used its solution in equation (4) to resolve it.

Parameters H_g , n , k_s and η were calibrated by comparing the simulated and measured water contents. Parameter λ was calibrated by comparing the simulated and measured bromide concentrations, while k_d , μ_s and μ_w were calibrated by comparing the simulated and measured concentrations of carbofuran.

The calibration was done by minimizing the RMSE error between measurement and simulation:

$$\text{RMSE} = \frac{1}{O_{\text{moy}}} \sqrt{\frac{1}{N} \sum_{i=1}^n (S_i - O_i)^2} \quad (13)$$

where S_i is the model prediction, O_i is the observation, O_{moy} is the observation average and n is the total number of observations.

3. Results and discussion

3.1. Retention curve $\theta(h)$ and hydraulic conductivity $K(h)$

After several infiltrometer measurements at different pressures, we were able to reconstruct a part of the retention curve $\theta(h)$ (Fig. 2), the value θ_r was taken equal to zero, since the soil is very sandy and has a very low capacity to retain water in dry-state conditions. In Fig. 2, the experimental points are aligned with the fitted curve, hence justifying our choice of Van Genuchten's model (Van Genuchten, 1980). The results of this adjustment are presented in Table 2.

Table 2

Values and standard deviation of the parameters of the Van Genuchten model $\theta(h)$ and the Brooks–Correy model $K(h)$ adjusted to fit the experimental values.

	Value	Standard deviation
θ_s (cm ³ /cm ³)	0.431	0.007
m	0.156	0.032
n	2.36	0.09
h_g (cm)	-2.73	0.96
K_s (cm/s)	0.0089	0.0005
η	5.9	0.9

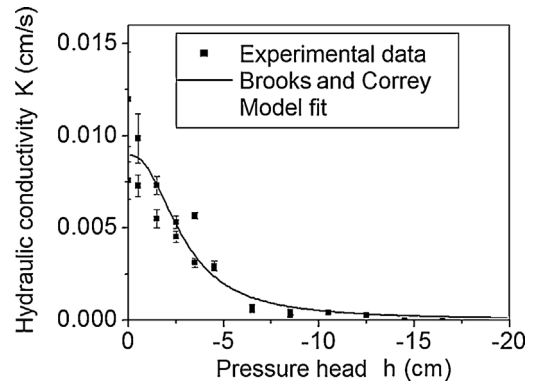


Fig. 3. $K(h)$ curve for the studied soil.

The measured $K(h)$ during infiltration (Fig. 3) has a less dispersed curved shape. Table 2 shows the values of K_s and η obtained by fitting the Brooks and Corey model (Brooks and Corey, 1964) onto the measurement points; these values are close to the average values measured at Mnasra (Saâdi and Maslouhi, 2003).

It should be noted that the adjustment of Figs. 2 and 3 was carried out following the Levenberg–Marquardt Algorithm (LMA). The shape parameter η is often estimated in the literature as $(2 + 3L)/L$, where $0.2 < L < 3$ (Løvoll et al., 2011); in our case, the L value was 0.7. The η value estimated in this study, comprised between 5.8 and 7.4, is very close to the results of Saâdi et al. (1999) and Tamoh and Maslouhi (2004) in the coastal part of Mnasra.

3.2. The water movement

Solving Richard's equation yields solutions in h , which are converted into water content via relation $\theta(h)$. Simulations show that the water content of the soil could never mathematically go below its residual value θ_r , even if the internal evaporation phenomenon is taken into consideration. This confirms our consideration of an almost null residual water content (Bagarello and Iovino, 2012; Coppola et al., 2009; Mubarak et al., 2009; Saâdi and Maslouhi, 2003; Tamoh and Maslouhi, 2004). Moreover, considering the residual water content as null when it is very small allows us to cut down the number of parameters to be calibrated, and therefore to avoid over-parameterization. We performed a sensitivity analysis of the model results with respect to different values of the residual water content assigned to $\theta_r = 0.02, 0.04, 0.06$. We found that the variation of the residual water content has only a very limited impact on the mass balance of carbofuran effect.

We measured and simulated water content profiles during three months at three soil depths, i.e., 0–20, 20–40, and 40–60 cm. The volumetric water content is characterized by small variations, especially in the lower depths. It is due to the soil sandy texture, characterized by low retention capacity, a potential drainage, and low initial volumetric water content (see Fig. 4). Fig. 4A shows that the model simulations are in good agreement with the

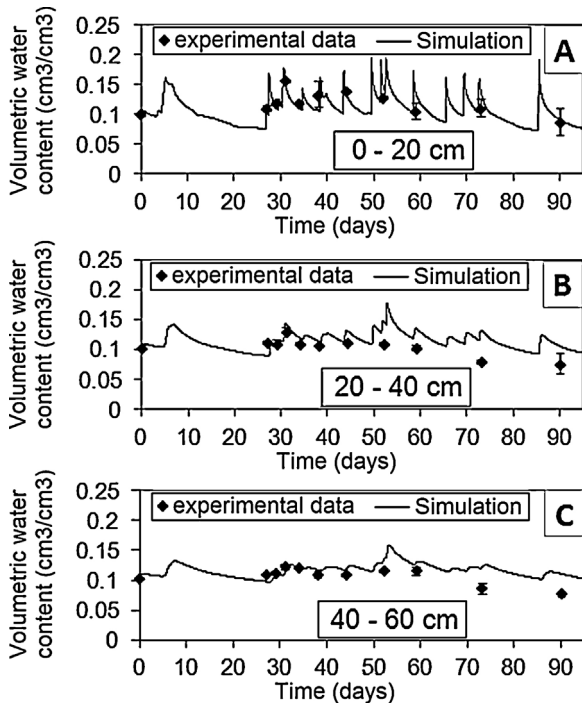


Fig. 4. Water content numerical simulations and experimental data at different soil depths.

experimental observations. In Fig. 4 B and C, the observed values are simulated with only a slight overestimation for the last sampling dates, probably due to the heterogeneity of the soil or error-related measurements.

The calibration error of h_g , m and η parameters (RMSE) gives a satisfactory value of 0.09 (Table 3). The k_s variation, within the limits of possible values for a soil like ours, does not affect the simulation results and, therefore, the value of RMSE. This allows us to consider that the hydrodynamic parameters are well represented. Furthermore, we find out that the model gives good predictions of the water content values, especially on the 0–20-cm profile.

3.3. Bromide transport

Fig. 5 shows the temporal evolution of bromide concentrations for the three soil horizons studied. Therefore, the dispersivity value λ is 0.115 m (Table 3). The fact that the value of λ seems high may be due to physical

Table 3
Values of calibrated hydrodynamic parameters and parameters λ , K_d , μ_s , and μ_w , with calibration errors.

	Value	Calibration error (RMSE)
h_g (cm)	-2.9	
n	2.34	0.09
η	7.2	
λ (cm)	11.5	0.48
K_d (cm ³ /g)	0.21	
μ_s (s ⁻¹)	2.10 ⁻⁷	0.54
μ_w (s ⁻¹)	2.10 ⁻⁷	

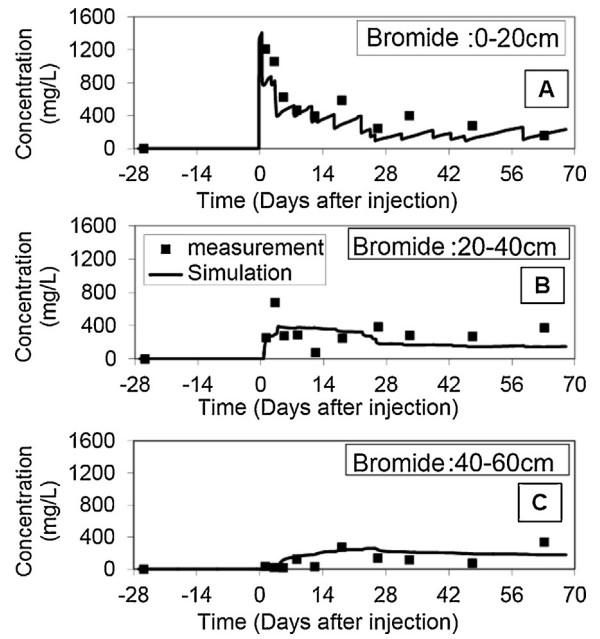


Fig. 5. Bromide concentration numerical simulations and experimental data at different soil depths.

phenomena neglected during modelling, including the three-dimensional nature of the flow across the field, the soil heterogeneity along the vertical profile, and the presence of preferential flows.

However, such a λ value is not surprising (Saâdi and Maslouhi, 2003), since according to the work of Nielsen et al. (1986), λ can take values ranging from 0.05 cm in a laboratory test, to 10 cm and higher for field conditions.

Table 3 shows an irrelevant $\lambda = 0.48$ value of the calibration error (RMSE), which is due to a slight fluctuation of the calculated values in the soil layers, especially in the lower ones. Nevertheless, the model yields results consistent with the observations. The calibration method seems therefore qualitatively acceptable, even for a heterogeneous soil.

3.4. Carbofuran transport

Simulated and observed concentrations of carbofuran, for levels 0–20 cm, 20–40 cm, and 40–60 cm are shown in Fig. 6. A few days after application, and after 25 days of leaching, carbofuran is practically distributed throughout the soil matrix, and the maximum rate of recovery is in the 0–20 cm layer. This observation suggests the existence of important phenomena of dispersion on the sandy substrate, which appear more pronounced on the topsoil horizon. The adsorption process is probably related to a slight increase in the organic matter content in this level (Table 1).

In addition, the model provides satisfactory results in terms of pesticide dynamics, except for the increase of the RMSE calibration error to 0.54 (Table 3). This increase is probably due to changes in distribution coefficients K_d and to μ degradation in each layer. Bearing in mind that we

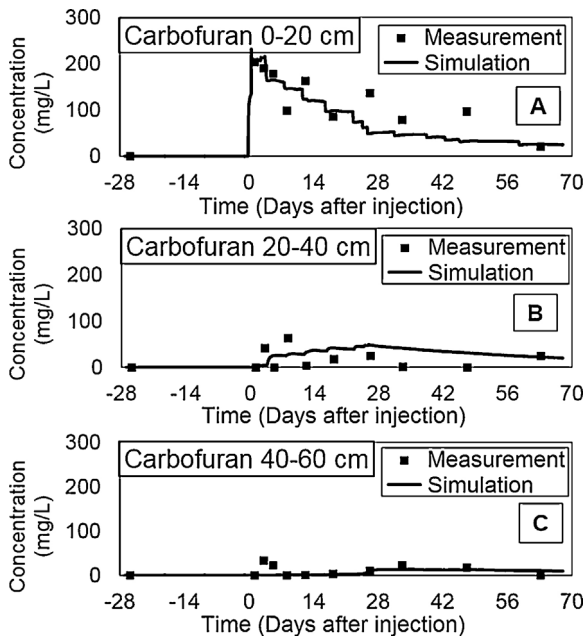


Fig. 6. Carbofuran concentration numerical simulations and experimental data at different soil depths.

considered a homogeneous soil as the modelling approach, the physicochemical characteristics of the pesticide were the same in all soil profiles, whereas the soil is actually heterogeneous. The values of the rate of degradation (μ_s and μ_w) inferred by calibration, and those calculated by the equation ($\mu_s = \mu_w = \ln 2 / t_{1/2} = 0.693 / t_{1/2}$) (Sparks, 1989) show some similarities, as the half-life ($t_{1/2}$) of carbofuran derived from a previous study for a sandy soil similar to our soil gave a similar carbofuran half-life (El Mrabet, 2002).

Differences observed between simulated and measured concentrations are probably due to the following reasons:

- errors in experimental measurements;
- influence of other physical phenomena related to transport not considered in modeling;
- we considered 1D model approach, whereas the real phenomena are in 3D.

It is appropriate to specify that the volatilization is not considered, since carbofuran has low volatility and is characterized by a low vapor pressure (3.41×10^{-6} mmHg at 25 °C). According to Lardier (Lardier, 1987), the volatilization of carbofuran is limited to 0.5% for sandy soils after two months of treatment.

A sensibility analysis shows little influence of θ_r on the water movement, and to a lesser degree, on carbofuran mass balance, especially on the carbofuran leaching flux.

Therefore, we used the model developed to simulate the transport of carbofuran for two different irrigation regimes, i.e., 222 mm and 350 mm. Fig. 7A and B present the simulation results of carbofuran transport in the unsaturated soil down to a 1-m depth in both irrigation schemes (222 mm and 350 mm) area. Fig. 7 shows the

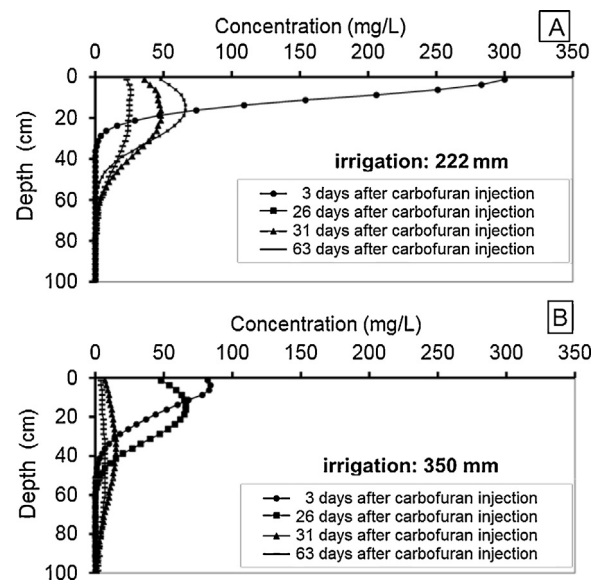


Fig. 7. Simulations of carbofuran distribution in the soil following two irrigation regimes (A: 222 mm; B: 350 mm).

distribution of the pesticide 3, 26, 31, and 63 days after application.

According to both irrigation regimes, the maximum carbofuran concentration in soil reaches 300 mg/L and 84 mg/L, respectively. These peaks appear three days after carbofuran surface application. We can observe a decrease in the maximum concentration and a slight advance of the concentration front according to the increase of irrigation amount. The same phenomenon is observed for these concentration profiles 26 days after treatment.

The two profile graphs of carbofuran concentrations appearing 31 and 63 days after application are flat and wide, including the largest irrigation system (Fig. 7B). The curves show that the dispersive transport is enhanced by irrigation. The analysis of the results shows some migration of carbofuran down into in soil. The downward movement of carbofuran is more pronounced in Fig. 7B, which coincides with the increase in irrigation, i.e., 350 mm in total. The carbofuran mobility is also facilitated by its high solubility in water, i.e., 700 mg/L, and the large amounts of water provided by the irrigation system.

4. Conclusion

We carried out an experimental and numerical study in order to improve our knowledge and understanding of the mobility of a pesticide in a soil, namely carbofuran, which has a broad application spectrum. The study is focused on the mobility of carbofuran in soils with strong hydraulic permeability and characterized by a weak organic matter content. The model developed for this study favorably reproduced the magnitude and the general trend of the spatio-temporal evolution of water content and carbofuran concentration in the soil. It was therefore used to simulate the transport of carbofuran in the same experimental conditions using higher irrigation level, i.e.,

350 mm in total. The results of such simulations highlighted the importance of irrigation methods on the leaching of carbofuran especially to shallow groundwater: waters will be exposed to higher contamination for huge irrigation systems or during rainy periods. The migration of carbofuran residues and degradation products will be improved in the case of intensive crops treatment, which heavily depends on irrigation water such as gardening, banana plantation, etc., leading to faster and larger transports.

Overall, these data indicate that aquifers with an underlying unsaturated sandy zone characterized by a low clay content and soil organic matter are particularly vulnerable to carbofuran contamination. This is particularly true for drinking water after heavy rainfall or irrigation, and all the more after unsound repetitive pesticide applications. This problem requires in the future a more detailed study of carbofuran leaching on other soil types. It is also important to integrate the entire crop cycle, the effect of land-use change that may affect soil content in clay (Cornu et al., 2012) and, consequently, the leached quantity of carbofuran and the effect of pesticide dose. In addition, the contamination by the major metabolites caused by the carbofuran degradation, i.e., carbofuran phenol, 3-hydroxy-carbofuran, and 3-keto-carbofuran will have to be evaluated in details in the future. They are known to have similar toxicity to the original compound, and their solubility in water is greater than that of carbofuran (El Mrabet, 2002).

References

- Bagarello, V., Iovino, M., 2012. Testing the BEST procedure to estimate the soil water retention curve. *Geoderma* 187–188, 67–76.
- Beven, K.J., 2012. Causal models as multiple working hypotheses about environmental processes. *C. R. Geoscience* 344, 77–88.
- Brooks, R.H., Corey, C.T., 1964. Hydraulic properties of porous media. *Hydro. Paper 3*. Colorado State University, Fort Collins.
- Candela, L., Mariño, M., 2004. Simulation of 2,4-D herbicide transport through the unsaturated zone using an analytical model. *Intern. J. Environ. Anal. Chem.* 84 (1–3), 123–131.
- Coppola, A., Basile, A., Comega, A., Lamaddalena, N., 2009. Monte Carlo analysis of field water flow comparing uni- and bimodal effective hydraulic parameters for structured soil. *J. Contam. Hydrol.* 104, 153–165.
- Cornu, S., Montagne, D., Hubert, F., Barré, P., Caner, L., 2012. Evidence of short-term clay evolution in soils under human impact. *C. R. Geoscience* 344, 747–757.
- Dahchour, A., 1995. Studies on the behaviour of nematicides in soil under banana cultivation in Morocco PhD. Univ. London, 165 p.
- El Mrabet, M., 2002. Contribution à l'étude de l'adsorption du carbofuran et du phénamiphos par les complexes argilo-humiques et par les sols et de la biodégradation du carbofuran. Thèse, Université Ibn-Tofail, Kénitra.
- Gustafson, D.I., 1989. Groundwater ubiquity score: a simple method for assessing pesticides leachability. *Environ. Toxicol. Chem.* 8, 339–357.
- Hmimou, A., Candela, L., Queralt, I., Tamoh, K., Maslouhi, A., 2011. X-ray fluorescence analysis for total bromine tracking in vadose zone: results for Mnasra, Morocco. *Vadose Zone J.* 10, 1–5.
- Ibnoussina, M., El Haroui, M., Maslouhi, A., 2006. Expérimentation et modélisation de la lixiviation de l'azote nitrique dans un sol sableux. *C. R. Geoscience* 338, 787–794.
- Kodešová, R., Kočárek, M., Kodeš, V., Drábek, O., Kozák, J., Hejtmánková, K., 2011. Pesticide adsorption in relation to soil properties and soil type distribution in regional scale. *J. Hazard. Mater.* 186, 540–550.
- Krishna, K.R., Philip, L., 2008. Adsorption and desorption characteristics of lindane, carbofuran and methyl parathion on various Indian soils. *J. Hazard. Mater.* 160 (2–3), 559–567.
- Kuntz, D., Grathwohl, P., 2009. Comparison of steady-state and transient flow conditions on reactive transport of contaminants in the vadose soil zone. *J. Hydrol.* 369, 225–233.
- Laftouhi, N., Vanclooster, M., Jalal, M., Witam, O., Aboufirassi, M., Bahir, M., Persoons, E., 2003. Groundwater nitrate pollution in the Essaouira Basin (Morocco). *C. R. Geoscience* 335, 307–317.
- Lardier, P., 1987. De la synergie entre insecticide et herbicide : cas du carbofuran et l'atrazine Thèse. Institut national polytechnique de Lorraine, Nancy, France.
- Løvoll, G., Jankov, M., Måløy, K.J., Toussaint, R., Schmittbuhl, J., Schäfer, G., Méheust, Y., 2011. Influence of viscous fingering on dynamic saturation–pressure curves in porous media. *Transport Porous Media* 86, 305–324.
- Margui, E., Queralt, I., Van Grieken, R., 2009. X-ray fluorescence analysis sample preparation for. In: Meyers, R.A. (Ed.), *Encyclopedia of analytical chemistry*. John Wiley & Sons, Chichester, UK, pp. 1–20.
- Moreau, A., Van bladel, R., 1983. Dynamique en sol structuré du carbofuran vers les nappes. *Med. Fac. Land. Rijk. Genot.* 48 (4), 985–995.
- Mubarak, I., Mailbol, J.C., Angula-Jaramillo, R., Ruelle, P., Boivin, P., Khaledian, M., 2009. Temporal variability in soil hydraulic properties under drip irrigation. *Geoderma* 150, 158–165.
- Nielsen, D.R., van Genuchten, M., Biggar, T.J.W., 1986. Water flow and solute transport processes in the unsaturated zone. *Water Resour. Res.* 22 (9), 89s–108s.
- Perroux, K.M., White, L., 1988. Design for disc permeameters. *Soil Sci. Soc. Amer. J.* 52, 1205–1215.
- Rekolainen, S., Gouy, V., Francaviglia, R., Eklo, M., Bärlund, O.I., 2000. Simulation of soil water, bromide and pesticide behaviour in soil with the GLEAMS model. *Agric. Water Manage.* 44, 201–224.
- Russo, D., Zaidel, J., Laufer, A., 1994. Stochastic analysis of solute transport in partially saturated heterogeneous soil, 2, prediction of solute spreading and breakthrough. *Water Resour. Res.* 30, 781–790.
- Saâdi, Z., Maslouhi, A., 2003. Modeling nitrogen dynamics in the unsaturated soils for evaluating the nitrate contamination of the Mnasra groundwater. *Adv. Environ. Res.* 7 (4), 803–823.
- Saâdi, Z., Maslouhi, A., Zeraoui, M., Gaudet, J.-P., 1999. Analyse et modélisation des variations saisonnières des concentrations en nitrates dans les eaux souterraines de la nappe de Mnasra, Maroc. *C. R. Acad. Sci. Paris Ser. Ila* 329, 579–585.
- Soil Survey Staff, 1999. Soil taxonomy 436 p. In: *A Basic System of Soil Classification for making and interpreting Soil Surveys*. US Dep. of Agriculture, Agriculture Handbook, Washington.
- Sparks, D.L., 1989. Kinetics of soil chemical processes. Academic Press, San Diego, CA, USA.
- Tamoh, K., Maslouhi, A., 2004. Mesures in situ par infiltrométrie des propriétés hydrodynamiques des sols de Mnasra-Maroc. *C. R. Geoscience* 336, 535–545.
- Tejón, G., Candela, L., Tamoh, K., Molina-Díaz, A., Fernández-Alba, A.R., 2010. Occurrence of emerging contaminants, priority substances (2008/105/CE) and heavy metals in treated wastewater and groundwater at Depurbaix facility (Barcelona, Spain). *Sci. Total Environ.* 408, 3584–3595.
- Tirumalesh, K., 2008. Simultaneous determination of bromide and nitrate in contaminated waters by ion chromatography using amperometry and absorbance detectors. *Talanta* 74, 1428–1436 doi:10.1016/j.talanta.09-021.
- USDA-SCS, 1975. Soil Taxonomy: A basic system of soil classification for making and interpreting soil surveys. U S Department of Agriculture, Soil Conservation Service, Soil Survey Staff, Agriculture Handbook No 436, Washington, DC.
- Van Genuchten, M.T., 1980. A closed-form equation for predicting the hydraulic conductivity of unsaturated soils. *Soil Sci. Soc. Am. J.* 44, 892–898.
- Worral, F., Kolpin, D.W., 2004. Aquifer vulnerability to pesticide pollution-combining soil, land-use and aquifer properties with molecular descriptors. *J. Hydrol.* 29 (1–4), 191–204.